

TeLL-Drive: Enhancing Autonomous Driving with Teacher LLM-Guided Deep Reinforcement Learning

Chengkai Xu, Jiaqi Liu, *Student Member, IEEE*, Peng Hang, *Senior Member, IEEE*, and Jian Sun

Abstract—Although Deep Reinforcement Learning (DRL) and Large Language Models (LLMs) each show promise in addressing decision-making challenges in autonomous driving, DRL often suffers from high sample complexity, while LLMs have difficulty ensuring real-time decision making. To address these limitations, we propose TeLL-Drive, a hybrid framework that integrates an Teacher LLM to guide an attention-based Student DRL policy. By incorporating risk metrics, historical scenario retrieval, and domain heuristics into context-rich prompts, the LLM produces high-level driving strategies through chain-of-thought reasoning. A self-attention mechanism then fuses these strategies with the DRL agent’s exploration, accelerating policy convergence and boosting robustness across diverse driving conditions. Our experimental results, evaluated across multiple traffic scenarios, show that TeLL-Drive outperforms existing baseline methods, including other LLM-based approaches, in terms of success rates, average returns, and real-time feasibility. Ablation studies underscore the importance of each model component, especially the synergy between the attention mechanism and LLM-driven guidance. These findings suggest that TeLL-Drive significantly enhances both the adaptability and safety of autonomous driving systems, while offering a more efficient and scalable approach for policy learning. Full validation results are available on Our Website.

I. INTRODUCTION

Autonomous driving technology has made significant advancements over the past decade, emerging as a transformative force poised to revolutionize the transportation sector [1]. By promising enhanced safety, reduced traffic congestion, and increased mobility accessibility, autonomous vehicles (AVs) are set to redefine the landscape of modern transportation. Central to the operational efficacy of AVs is their ability to perform real-time, complex decision-making that rivals or surpasses human driving capabilities. Achieving such sophisticated decision-making necessitates the integration of advanced artificial intelligence methodologies capable of perceiving, interpreting, and responding to dynamic and often unpredictable driving environments [2].

Deep Reinforcement Learning (DRL) has become a key framework for decision-making in autonomous systems [3], [4]. In autonomous driving, DRL is used to develop policies for vehicle behaviors, such as intersection navigation [5]. However, traditional DRL faces challenges, including high data requirements, slow convergence, and limited environmental understanding [6], hindering its scalability and efficiency in dynamic driving scenarios that demand robust adaptability.

C.Xu, J.Liu, P.Hang and J.Sun are with the Department of Traffic Engineering and Key Laboratory of Road and Traffic Engineering, Ministry of Education, Tongji University, Shanghai 201804, China.(e-mail: xck1270157991@gmail.com, liujiaqi13, hangpeng, sunjian@tongji.edu.cn)

Corresponding author: Peng Hang

Concurrently, LLMs, exemplified by architectures such as GPT-4, have demonstrated exceptional proficiency in understanding and generating human-like text. Leveraging vast repositories of knowledge and advanced contextual reasoning capabilities, LLMs have been applied to decision-making processes in autonomous driving [7]–[9]. However, their practical deployment as standalone decision-making agents is constrained by inherent challenges [10]. Specifically, LLMs struggle to ensure real-time responsiveness and exhibit a degree of randomness in their decision outputs, which are critical limitations in time-sensitive and safety-critical applications inherent to autonomous driving systems.

To address these challenges, we propose **TeLL-Drive**, a framework that synergistically combines the strengths of DRL and LLMs to enhance decision-making in autonomous vehicles. TeLL-Drive mitigates the inherent limitations of DRL and LLMs by leveraging the contextual understanding and reasoning capabilities of LLMs to improve the sampling efficiency and quality of the DRL process. Specifically, we develop a risk-aware LLM agent equipped with memory, reflection, and reasoning abilities, enabling efficient and safe decision-making in complex traffic environments. Meanwhile, a DRL agent based on the Actor-Critic architecture is designed, which employs hybrid strategies to enhance sampling efficiency and quality while preserving robust exploration capabilities.

As shown in Fig. 1, LLMs function as “teachers”, providing high-quality guidance and contextual insights that inform and streamline the learning process of DRL agents. Subsequently, DRL serves as the “student”, acting as the final decision maker to ensure real-time responsiveness and mitigate the randomness associated with LLM-driven decisions. The main contributions of this article are listed as follows:

- 1) TeLL-Drive is proposed, a novel framework for autonomous driving decision-making that combines a “teacher” LLM with a “student” DRL agent, which integrates the LLM’s high-level reasoning and knowledge with DRL’s adaptability and computational efficiency.
- 2) A risk-aware LLM agent is developed, which is endowed with memory, reflection, and reasoning capabilities, to provide context-sensitive guidance in dynamic traffic environments and enhance driving safety and efficiency.
- 3) Through experiments in multiple scenarios, TeLL-Drive outperforms standard DRL algorithms in exploration efficiency and achieves favorable overall results compared to alternative methods.

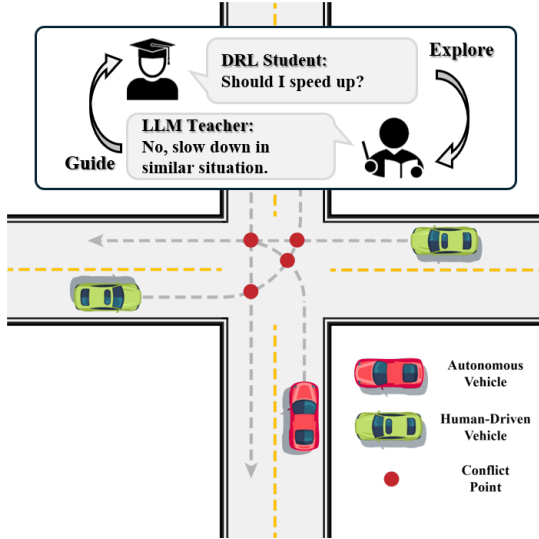


Fig. 1. The LLM teacher guides the DRL agent in decision-making within complex traffic scenarios, offering corrective feedback during exploration to enhance learning efficiency and decision-making accuracy.

II. RELATED WORKS

A. DRL for Autonomous Driving Decisions

DRL has shown strong potential in autonomous driving, spanning tasks from lane-keeping to complex multi-agent interactions [11], [12]. However, two main challenges remain. Firstly, DRL often requires extensive environment interactions, which is costly and time-consuming. Secondly, lack of transparency impedes reliable decision-making in rare or out-of-distribution scenarios. To mitigate these issues, Reinforcement Learning from Human Feedback (RLHF) [13] has been proposed to incorporate expert knowledge, accelerating convergence and improving policy robustness. Nonetheless, RLHF remains costly due to the extensive human annotations required [14], and its feedback may not cover all possible driving conditions.

B. LLMs in Decision-Making

LLMs have exhibited significant promise in various tasks, including high-level reasoning for autonomous driving [15]. For instance, LanguageMPC [16] leverages an LLM’s common-sense reasoning to guide Model Predictive Control parameters, while Fu et al. [17] and Wen et al. [18] demonstrate LLM-based reasoning, interpretation, and memory capabilities for driving decisions. Despite these advances, direct deployment of LLMs faces obstacles. While high computational overhead makes LLMs difficult to achieve rapid, consistent responses required for safe driving, stochastic text generation may lead to unpredictable actions, which is risky in safety-critical environments.

C. Hybrid RL-LLM Approaches

There is growing interest in combining RL and LLMs, though most efforts focus on using RL to refine LLMs rather than leveraging LLMs to enhance RL—particularly for

autonomous driving. Initial studies have shown the potential of LLM-based reasoning to improve exploration efficiency and learning effectiveness of RL [19]. For example, Zhang et al. [20] introduced a semi-parametric RL framework with LLM-driven long-term memory, Trirat et al. [21] employed LLMs for automated machine learning, and Ma et al. [22] automated RL reward function design. However, fully exploiting LLMs for environmental understanding and decision-making in autonomous driving remains an open challenge, as existing approaches lack a systematic integration strategy that fully harnesses LLMs’ knowledge and reasoning capabilities.

III. PROBLEM FORMULATION

We formalize the autonomous driving decision-making task as a Partially Observable Markov Decision Process (POMDP), defined by the tuple $\langle \mathcal{S}, \mathcal{A}, \mathcal{O}, \mathcal{T}, \mathcal{R}, \gamma \rangle$, where \mathcal{S} is the environmental states; \mathcal{A} is the action space; \mathcal{O} is the observation space; \mathcal{T} is the state transition function; \mathcal{R} is the reward function, and γ is the discount factor. The agent’s objective is to learn a policy π that maximizes the expected discounted return:

$$\max_{\pi} J(\pi) = \arg \max_{\pi} \mathbb{E}_{(s_t, a_t) \sim \rho_{\pi}} \left[\sum_{t=0}^{\infty} \gamma^t r(s_t, a_t) \right] \quad (1)$$

where $\gamma \in [0, 1]$ balances the emphasis on immediate and future rewards.

1) *Observation space*: At each time step t , the agent receives an observation $o_t \in \mathcal{O}$ composed of two parts. The first is a matrix $M_t \in \mathbb{R}^{\mathcal{F}_k \times N}$ capturing information about up to N nearby vehicles. Each column of M_t corresponds to one vehicle, described by a feature vector:

$$\mathcal{F}_k = [x_k, y_k, v_{x_k}, v_{y_k}, \cosh(\theta_k), \sinh(\theta_k)] \quad (2)$$

where (x_k, y_k) and (v_{x_k}, v_{y_k}) denote the position and velocity of the k -th vehicle, and $\cosh(\theta_k)$ and $\sinh(\theta_k)$ encode its orientation. The second part of o_t is the state of the ego vehicle. By concatenating these components, the agent obtains a compact yet informative representation of the driving environment.

2) *Action space*: This work focuses on leveraging LLMs to provide high-level guidance for DRL, rather than controlling low-level vehicle dynamics. Consequently, the action space \mathcal{A} consists of five high-level maneuvers: $\{\text{slowdown}, \text{cruise}, \text{speedup}, \text{turnleft}, \text{turnright}\}$. Once a high-level maneuver is chosen, the corresponding steering and throttle commands are generated by a lower-level PID controller, enabling the vehicle to execute lateral and longitudinal movements.

IV. METHODOLOGY

A. Framework overview

TeLL-Drive leverages the knowledge of LLMs to guide the exploration and learning of DRL agents in various traffic scenarios. By introducing policy mixing, TeLL-Drive enhances sample efficiency and optimizes learning outcomes. As illustrated in Fig. 2, the framework comprises two main components: the *LLM Teacher* and the *DRL Student*. Based on multi-module collaboration, the Teacher Agent generates robust

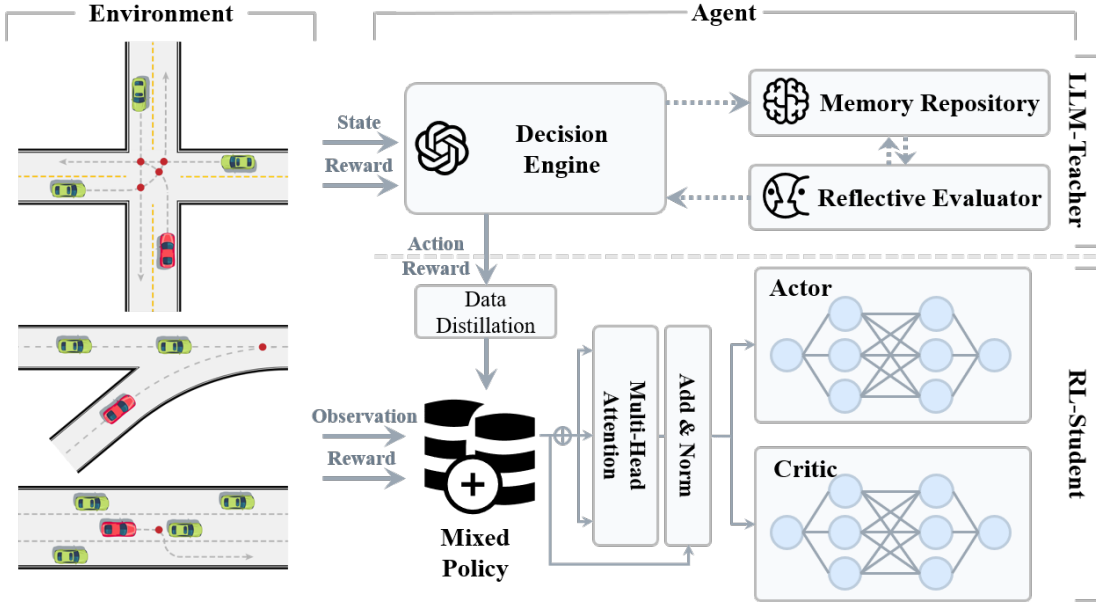


Fig. 2. The overall conceptual framework of TeLL-Drive, where a DRL student agent is guided by the LLM teacher for better decision making in autonomous driving.

decision in complex traffic scenarios. The Teacher Agent generates robust decisions through its three key modules: *Decision Engine*, which provides real-time guidance; *Memory Repository*, which stores past experiences for context; and *Reflective Evaluator*, which refines the guidance based on previous performance. While the Student Agent refines the Teacher’s actions through a multi-head attention-based policy-mixing mechanism, integrating its own exploration experiences to effectively acquire knowledge from the LLM and enhance learning efficiency and quality.

B. LLM Teacher

1) **Decision Engine**: The Decision Engine begins by estimating the Time to Conflict Point (TTCP) [15] for each potential collision, using a rotation-projection method that projects the relative motion vectors of the ego vehicle and other traffic participants onto a shared reference axis. Let $\mathbf{d}_{\text{ego}}(t)$ and $\mathbf{d}_{\text{other}}(t)$ be the positions of the ego and another vehicle at time t , $v_{\text{ego}}(t)$ and $v_{\text{other}}(t)$ be the current speed. The TTCP τ is:

$$\tau = \arg \min_{t \geq 0} \left\| \frac{\mathbf{p}_{\text{ego}}(t)}{v_{\text{ego}}(t)} - \frac{\mathbf{p}_{\text{other}}(t)}{v_{\text{other}}(t)} \right\| \quad (3)$$

This risk metric informs immediate maneuver priorities. Simultaneously, we retrieve context from a memory repository indexing historical driving scenarios as feature vectors $\{\mathbf{z}_i\}$. For the current state $\mathbf{z}_t \in \mathbb{R}^d$, we retrieve the most similar scenario \mathbf{z}_i via cosine similarity, thus leveraging outcomes of analogous past experiences to guide decision-making:

$$\text{sim}(\mathbf{z}_t, \mathbf{z}_i) = \frac{\mathbf{z}_t \cdot \mathbf{z}_i}{\|\mathbf{z}_t\| \|\mathbf{z}_i\|} \quad (4)$$

Building on these real-time and historical insights, the engine constructs a comprehensive prompt \mathcal{P}_t that integrates TTCP-derived risks, scenario-specific experiences, and traffic

knowledge. This prompt includes road geometry, vehicle positions, and conflict zones, along with domain heuristics to provide the LLM with a rich contextual foundation for action proposals. To enhance reliability and minimize hallucinations, we then employ a chain-of-thought approach in which the model iteratively evaluates collision severity, short- and long-term maneuver consequences, and broader traffic implications. This structured reasoning process reduces logical inconsistencies, resulting in safer and more interpretable autonomous driving policies.

2) **Memory Repository**: The Memory Repository stores and manages all pertinent knowledge required by the LLM Teacher. It operates as a dynamic database \mathcal{M} that contains the prior scenarios and policies, which includes the historical states $\{\mathbf{s}_i\}$, actions $\{\mathbf{a}_i\}$ and consequences $\{\mathbf{r}_i\}$.

When generating a new prompt \mathcal{P}_t , the Decision Engine queries \mathcal{M} for relevant context, ensuring the LLM has immediate access to historical examples and domain constraints. By selectively retrieving and embedding these elements, the LLM Teacher can provide more accurate and context-sensitive guidance:

$$\mathcal{P}_t \leftarrow \text{Retrieval}(\mathbf{s}_t, \mathcal{M}). \quad (5)$$

Periodic updates to \mathcal{M} occur based on newly encountered scenarios or reflective feedback from previous driving sessions. This design allows the LLM Teacher to accumulate knowledge over time, enabling improved reasoning and continuous evolution across diverse driving environments.

3) **Reflective Evaluator**: The Reflective Evaluator systematically reviews driving episodes to improve decision-making by identifying risky events and integrating learned lessons into future policies.

After each driving session, we first collect the experience tuples:

$$D = \{(s_t, a_t, s_{t+1}) \mid t = 1, 2, \dots, T\} \quad (6)$$

Algorithm 1: LLM Teacher Agent

Input : State $s(t)$, Memory \mathcal{M}
Output: Action $a_t \in A$

- 1 **for** $t \leftarrow 0$ **to** T_{max} **do**
- 2 **for** $i \leftarrow 1$ **to** $N_{vehicle}$ **do**
- 3 **Identify critical risks:**
- 4 $\tau_i = \arg \min_{\Delta t \geq 0} \|\mathbf{p}_{ego}(t + \Delta t) - \mathbf{p}_i(t + \Delta t)\|$
- 5 $\tau_{min} \leftarrow \min\{\tau_1, \dots, \tau_N\}$
- 6 **end**
- 7 **Construct Current State Vector:**
- 8 $\mathbf{z}_t \leftarrow (\mathbf{p}_{ego}(t), \mathbf{v}_{ego}(t), \{\mathbf{p}_i(t), \mathbf{v}_i(t)\}_{i=1}^N, \{\tau_i\}_{i=1}^N)$
- 9 **Memory retrieval with cosine similarity:**
- 10 $\hat{j} \leftarrow \arg \max_{1 \leq j \leq M} \frac{\mathbf{z}_t \cdot \mathbf{z}_j}{\|\mathbf{z}_t\| \|\mathbf{z}_j\|}$
- 11 Construct prompt $\mathcal{P}_t \leftarrow \text{Retrieval}(s_t, \mathcal{M})$
- 12 **CoT Reasoning:**
- 13 $\mathcal{A}_t \leftarrow \{\text{Decoding LLM final decision}\}$
- 14 **Reflective Evaluator Update:**
- 15 Calculate risk: $\Omega : \mathcal{S} \times \mathcal{A} \rightarrow \mathbb{R}^+$
- 16 **if** $\max_t \Omega(s_t, a_t) \geq \delta$ **then**
- 17 **Further Reflection:**
- 18 $\{\Delta Policy, \Delta Prompt, \Delta Constraint\} \leftarrow f_{LLM}(Q_{ref})$
- 19 **end**
- 20 $\mathcal{M} \leftarrow \text{Updated Memory after Reflection}$
- 21 **end**
- 22 **return** a_t, \mathcal{M}

where s_t and a_t denote the state and action at time t and s_{t+1} denotes the subsequent state. To pinpoint high-risk segments, we define a risk function $\Omega : \mathcal{S} \times \mathcal{A} \rightarrow \mathbb{R}^+$ that quantifies the potential for collisions or other undesirable outcomes.

$$\Omega(s_t, a_t) = \max\left(\frac{1}{\tau_{TTC P}(s_t, a_t)}, \beta \mathbb{I}\{infrac\}\right) \quad (7)$$

Any episode with $\max_t \Omega(s_t, a_t) \geq \delta$ is flagged for further reflection.

For the flagged segment $\{(s_i, a_i)\}_{i=k}^m$, the LLM is prompted to analyze the sequence of risky actions and causes. Through CoT reasoning, it proposes a domin-specific adjustment:

$$\{\Delta Policy, \Delta Prompt, \Delta Constraint\} \leftarrow f_{LLM}(Q_{ref}) \quad (8)$$

These updated constraints and policies are then integrated back into the memory repository \mathcal{M} and the decision engine's prompt construction logic. By iterating this reflection process, the LLM-Teacher systematically reduces error recurrence and strengthens overall policy robustness.

C. DRL student

1) **Actor-Critic Algorithm with Policy Constraint:** An actor-critic framework is adopted, where both the state-value function V^π and the action-value function Q^π are recursively estimated. For a policy $\pi(\mathbf{a} | \mathbf{s})$, the state-value function and the corresponding action-value function at state \mathbf{s}_t is:

$$V^\pi(\mathbf{s}_t) = \mathbb{E}_{\mathbf{a}_t \sim \pi(\cdot | \mathbf{s}_t)} [Q^\pi(\mathbf{s}_t, \mathbf{a}_t)] \quad (9)$$

$$Q^\pi(\mathbf{s}_t, \mathbf{a}_t) = r(\mathbf{s}_t, \mathbf{a}_t) + \gamma \mathbb{E}_{\mathbf{s}_{t+1} \sim T(\cdot | \mathbf{s}_t, \mathbf{a}_t)} [V^\pi(\mathbf{s}_{t+1})] \quad (10)$$

The goal of the algorithm is to determine the optimal policy π^* that maximizes $V^\pi(\mathbf{s})$ for all $\mathbf{s} \in \mathcal{S}$. In our proposed algorithm, we iteratively learn the V function and Q function by minimizing the mean-squared Bellman error (MSBE) and optimize the policy π by maximizing the Q value, where MSBE is defined as:

$$\mathcal{L}(\phi_i) = \mathbb{E}_{(\mathbf{s}_t, \mathbf{a}_t, r_t, \mathbf{s}_{t+1}) \sim \mathcal{B}} \left[(Q_{\phi_i}(\mathbf{s}_t, \mathbf{a}_t) - (r_t + \gamma V_g(\mathbf{s}_{t+1})))^2 \right] \quad (11)$$

where \mathcal{B} is the experience replay buffer, and V_g represents a periodically updated target value function. The actor network is optimized by selecting actions \mathbf{a}_t that maximize the critic's estimate $Q_{\phi_i}(\mathbf{s}_t, \mathbf{a}_t)$, thereby promoting higher return.

To incorporate demonstration actions from the LLM Teacher's policy π^T into the actor-critic framework and guide the DRL agent's policy π^S during early exploration, we introduce a Kullback–Leibler (KL) [23] divergence constraint. The agent's learning objective is formulated as a constrained optimization problem:

$$\begin{aligned} \min_{\pi^S} \mathbb{E}_{\mathbf{s}_t \sim \mathcal{D}} \mathbb{E}_{\tilde{\mathbf{a}}_t \sim \pi^S(\mathbf{s}_t)} [-Q_{\phi_i}(\mathbf{s}_t, \tilde{\mathbf{a}}_t)] \\ \text{s.t. } \hat{D}_{\text{KL}}(\pi^S(\mathbf{s}_t), \pi^T(\mathbf{s}_t)) \leq \sigma \end{aligned} \quad (12)$$

where $\sigma > 0$ is a tolerance that bounds the KL divergence between the agent's policy $\pi^S(\mathbf{s}_t)$ and the teacher's policy $\pi^E(\mathbf{s}_t)$. During early training, σ is kept small to enforce proximity to the teacher's demonstrated actions, thereby accelerating convergence. As training proceeds, σ gradually expands, allowing the agent to rely more on its own exploration while still incorporating early guidance. This procedure balances leveraging teacher knowledge for rapid initial learning with the agent's intrinsic exploration for robust final performance.

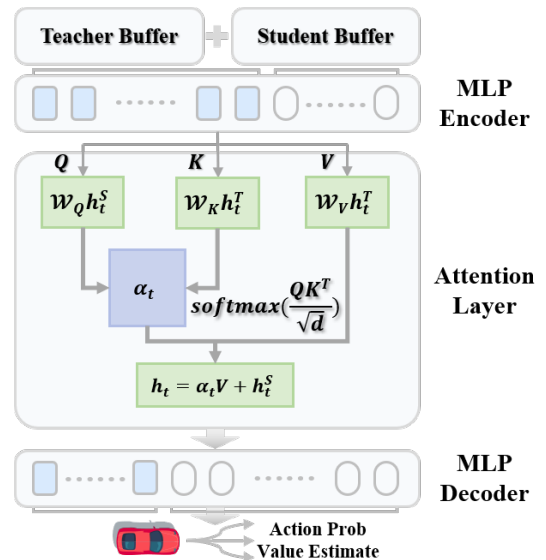


Fig. 3. Proposed policy network with self-attention layer. The network integrates self-attention to estimate action probabilities and value functions from the teacher's strategy, enabling strategy distillation and a balance between teacher guidance and self-exploration.

2) **Policy Distillation and Fusion:** Although the Teacher Agent offers high-level guidance, it does not directly provide action probabilities or value estimates. To bridge this gap, we embed a Transformer-based self-attention mechanism shown in Fig. 3 within the Student’s policy network. This component approximates the Teacher’s implicit policy and fuses it with the Student’s learned strategy in a flexible, data-driven manner.

Let $\mathbf{s}_t \in \mathcal{S}$ be the state at time t . We introduce two embeddings:

$$\mathbf{h}_t^S = f_S(\mathbf{s}_t), \quad \mathbf{h}_t^T = f_T(\mathbf{s}_t) \quad (13)$$

where f_S and f_T are neural encoders for the Student and the Teacher, respectively. The vector \mathbf{h}_t^T is learned to approximate the implicit Teacher policy, $\hat{\pi}^T$, and its corresponding action-value function, \hat{Q}^T . For each action $\mathbf{a} \in \mathcal{A}$:

$$\hat{\pi}^T(\mathbf{a} | \mathbf{s}_t) = \text{softmax}(\mathcal{W}_p \mathbf{h}_t^T + \mathbf{b}_p), \quad (14)$$

$$\hat{Q}^T(\mathbf{s}_t, \mathbf{a}) = \mathcal{W}_q \mathbf{h}_t^T + \mathbf{b}_q, \quad (15)$$

where $\{\mathcal{W}_p, \mathcal{W}_q, \mathbf{b}_p, \mathbf{b}_q\}$ are learnable parameters.

To integrate these dual embeddings, a self-attention mechanism is employed:

$$Q = \mathcal{W}_Q \mathbf{h}_t^S, \quad K = \mathcal{W}_K \mathbf{h}_t^T, \quad V = \mathcal{W}_V \mathbf{h}_t^T, \quad (16)$$

where $\mathcal{W}_Q, \mathcal{W}_K, \mathcal{W}_V$ are learnable projections. The self-attention coefficient α_t can be described as:

$$\alpha_t = \text{softmax}\left(\frac{QK^\top}{\sqrt{d}}\right) \quad (17)$$

with d denoting the dimensionality of K . The fused representation \mathbf{h}_t is:

$$\mathbf{h}_t = \alpha_t V + \mathbf{h}_t^S = \alpha_t \mathcal{W}_V \mathbf{h}_t^T + \mathbf{h}_t^S. \quad (18)$$

In multi-head settings, the process is replicated across several attention heads, and the outputs are concatenated.

The Student uses the fused embedding \mathbf{h}_t to produce its final policy $\tilde{\pi}$ and action-value estimate \tilde{Q} :

$$\tilde{\pi}(\mathbf{a} | \mathbf{s}_t) = \text{softmax}(\mathbf{W}_\pi \mathbf{h}_t + \mathbf{b}_\pi), \quad (19)$$

$$\tilde{Q}(\mathbf{s}_t, \mathbf{a}) = \mathbf{W}_Q \mathbf{h}_t + \mathbf{b}_Q, \quad (20)$$

The self-attention parameters and teacher embeddings are optimized jointly. If demonstration data $\{(s, \mathbf{a}_T)\}$ is available, an auxiliary distillation loss enforces consistency with the Teacher’s decisions:

$$\mathcal{L}_{\text{distill}} = -\mathbb{E}_{(s, \mathbf{a}_T) \in \mathcal{D}_T} [\log \hat{\pi}^T(\mathbf{a}_T | s)]. \quad (21)$$

This term encourages \mathbf{h}_t^T to distill excellent policies from the demonstrated behavior of the LLM Teacher, while the Student continues to learn its own policy through exploration and reward feedback.

V. EXPERIMENTS AND PERFORMANCE EVALUATION

A. Driving scenarios

We evaluate the comprehensive performance of our autonomous driving model using a gradient verification scenario constructed with Highway-Env [24] and OpenAI Gym. To capture a broad spectrum of driving complexities, we design

three heterogeneous task systems with progressively decreasing difficulty, as illustrated in Fig. 4:

- 1) **Unsignalized intersection (Fig. 4(a)):** The agent must execute an unprotected left turn at an unsignalized intersection, requiring conflict resolution and time-slot preemption to navigate crossing traffic safely.
- 2) **High-Speed Ramp Merging (Fig. 4(b)):** The agent operates on an acceleration lane, performing speed matching and gap selection to merge seamlessly into highway traffic at elevated velocities.
- 3) **Four-Lane Adaptive Cruise (Fig. 4(c)):** The agent focuses on fine-grained control of inter-vehicle distances and speeds across four lanes, highlighting precision in longitudinal control and continuous lane tracking.

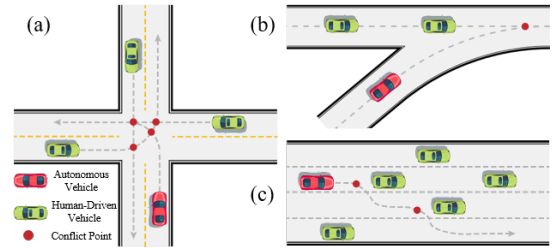


Fig. 4. The designed gradient verification scenario for simulation: (a) Unsignalized Intersection; (b) High-Speed Ramp Merging; (c) Four-Lane Adaptive Cruise.

By varying parameters, we simulate *conservative*, *standard*, and *aggressive* driver profiles, each featuring different desired speeds, accelerations, and tolerances for spacing. Vehicle speeds follow a normal distribution centered within a reasonable range, and we introduce a 15% abnormal speed disturbance to emulate real-world deviations.

B. Implementation Details

Both our model and the baseline methods utilize a policy network composed of a multilayer perceptron (MLP) with two hidden layers of size 128×128 . We employ two self-attention heads, each also of dimension 128, to fuse the Student and Teacher representations. We set the discount factor $\gamma = 0.99$ and adopt a learning rate of 5×10^{-4} . Each model is trained for at least 10^5 time steps, with an evaluation performed every 500 time steps. We use *GPT-4o-mini* as our LLM backbone, which shows reliable logical reasoning and real-time decision-making in driving tasks; it serves as the Teacher Agent for only the first 10% of training steps, after which constraints are gradually relaxed to encourage independent exploration. All experiments run on a computing platform equipped with Intel(R) Core(TM) i7-14700K CPU, an NVIDIA GeForce RTX 4080 SUPER GPU and 32 GB of RAM.

C. Performance Evaluation

1) **Comparison with Baseline Methods:** To assess the effectiveness of our approach, we benchmark four algorithms: a value-based method (DQN [25]), a policy-gradient method (A2C [26]), a sequence-memory-based method (RecurrentPPO [27]), and the current LLM-based state-of-the-art (Dilu [18]).

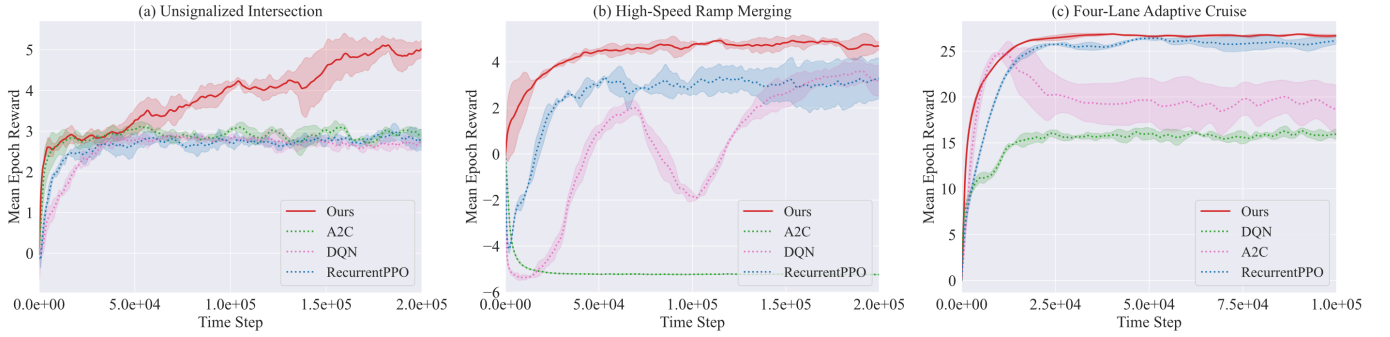


Fig. 5. Comparison of the performance of this model with traditional DRL training results.

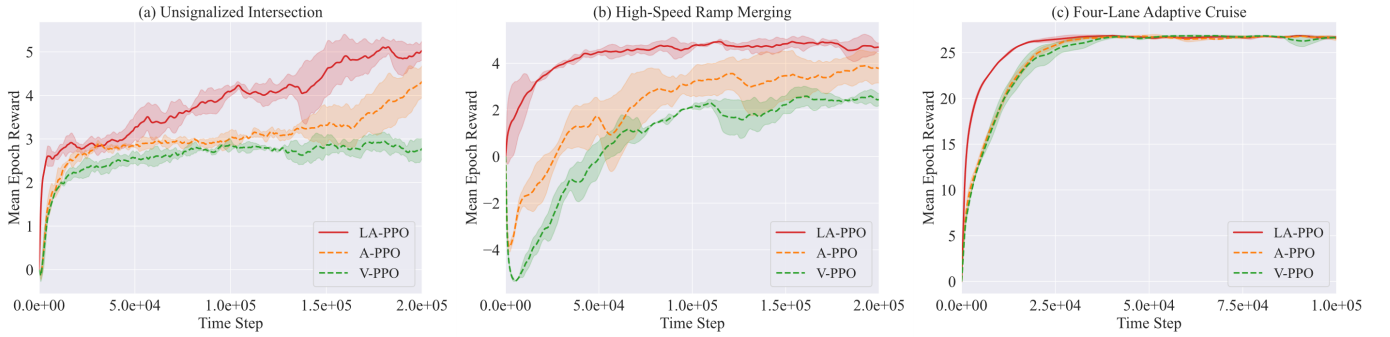


Fig. 6. Comparison of performance results during the ablation experiment training process.

TABLE I
COMPARISON OF SECURITY, EFFICIENCY, AND REAL-TIME TEST RESULTS OF DIFFERENT METHODS IN MULTIPLE SCENARIOS.

Scn	Model	Success Rate (%)	Eval Reward	Avg. Speed (m/s)	Δ TTCP (s)	Consumption Time (s)
Intersection	DQN	58	3.22	8.77	5.22	0.002
	A2C	54	2.88	9.02	5.05	0.003
	RecurrentPPO	74	0.86	5.34	4.98	0.003
	Dilu	57	6.59	7.32	1.53	3.906
	Ours	88	5.68	7.36	4.92	0.004
Merge	DQN	83	2.81	13.01	1.21	0.002
	A2C	0	-5.20	28.28	0.37	0.002
	RecurrentPPO	30	1.83	22.05	0.28	0.003
	Dilu	46	3.21	14.92	0.72	6.166
	Ours	91	5.60	16.50	1.31	0.004
Highway	DQN	71	22.02	21.96	1.96	0.002
	A2C	50	21.95	25.00	2.18	0.003
	RecurrentPPO	88	25.55	20.30	2.18	0.003
	Dilu	78	29.53	23.39	2.21	6.131
	Ours	100	27.17	23.53	2.13	0.003

We record the average return during training in Fig. 5, where the solid lines denote mean performance and the shaded regions indicate 95% confidence intervals.

In unsignalized intersection shown in Fig. 5(a), Our model rapidly improves during the initial training phase and converges to the highest final return. A2C exhibits significant fluctuations, implying instability near convergence. While other baselines eventually stabilize, their end-stage returns remain notably below ours, highlighting a substantial performance gap. As shown in Fig. 5(b), our method achieves high returns early on, stabilizing around 5×10^4 steps and consistently maintaining near-optimal performance thereafter.

In contrast, DQN starts with negative returns and steadily climbs to a suboptimal plateau. A2C fares the worst, likely owing to its sensitivity in time-critical merging tasks. Although RecurrentPPO converges more promptly than A2C, its ultimate reward remains below our model’s, underscoring the challenges of handling highly dynamic traffic with simple recurrent mechanisms. All methods experience rapid early gains, yet differ significantly in final returns and stability in Fig. 5(c). Our model maintains a leading position throughout and converges to a near-maximal reward. RecurrentPPO is intermittently competitive but prone to fluctuations. DQN and A2C both show moderate terminal performance, with A2C

stabilizing late but still achieving a lower reward ceiling.

What’s more, Table I provides a numerical summary of success rate, evaluation return, average speed, Δ TTCP, and decision-making time for each approach. In the unsignalized intersection scenario, our method attains the highest success rate (88%) while balancing speed and safety margins. For high-speed ramp merging, it achieves 91% success and outperforms the baselines in average return. Notably, A2C, despite having the highest speed, completely fails (0% success), demonstrating that overly aggressive driving sacrifices safety and thus overall performance. In four-lane adaptive cruise, our method reaches a perfect success rate (100%) alongside near-optimal speed and return. Although Dilu shows better speed and safety margins than traditional DRL methods, its extended reasoning time limits online deployment. Overall, our approach surpasses both conventional DRL algorithms and the LLM-based Dilu, underlining its effectiveness and robustness across diverse scenarios.

2) *Ablation Study*: To evaluate the impact of each component, we conduct an ablation study comparing *Vanilla PPO* (V-PPO [28]), *Attention-based PPO* (A-PPO), and our *LLM-Guided Attention PPO* (LA-PPO). As shown in Fig. 6, LA-PPO demonstrates faster convergence and higher final rewards relative to V-PPO and A-PPO, indicating superior stability and robustness. In the more demanding scenarios, such as unsignalized intersection and high-speed ramp merging, LA-PPO quickly attains higher returns and preserves its advantage throughout training. Although all methods converge to similar rewards in the simpler four-lane adaptive cruise task, LA-PPO still displays a slight edge in convergence rate and peak performance. These observations confirm that leveraging LLM guidance in conjunction with an attention mechanism yields more effective teacher knowledge transfer and better-directed policy learning.

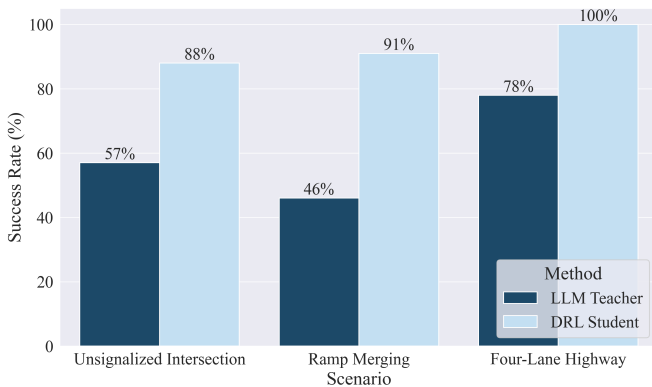


Fig. 7. Comparison of testing success rate results between the teacher agent and the student agent.

3) *Teacher-Student Comparison*: As shown in Fig. 7, we further examine success rates for the LLM Teacher and the DRL Student in each scenario. The Student outperforms the Teacher across all tasks, illustrating that while LLM guidance aids rapid early-stage learning, continual environment interaction empowers the Student to refine and ultimately surpass the Teacher’s performance. This outcome highlights the strengths

of a teacher-student paradigm in autonomous driving policy learning.

D. Case Analysis

To illustrate the model’s decision-making and behavioral patterns in realistic settings, Fig. 8 presents three representative cases. In Fig. 8(a), the agent carefully negotiates an unsignalized intersection, slowing at step 4 to yield and again decelerating at step 12 upon detecting oncoming traffic. Fig. 8(b) shows the agent merging onto a highway by accelerating, then briefly braking to maintain a safe following distance, and finally speeding up once the gap is sufficient. In the denser traffic scenario of Fig. 8(c), the agent continuously adapts its speed to preserve a safe headway despite flow disturbances. Taken together, these examples corroborate our quantitative results, evidencing the method’s efficacy in real-time decision-making, traffic interaction, and safety.

VI. CONCLUSION

Our proposed TeLL-Drive framework integrates teacher-guided learning with attention-based policy optimization, enabling efficient knowledge transfer and robust decision-making. Experimental results demonstrate that TeLL-Drive outperforms conventional DRL methods and existing LLM-based approaches across multiple metrics, including success rate, average return, and real-time feasibility. Additionally, ablation studies highlight the significance of each model component, particularly the synergy between attention mechanisms and LLM teacher guidance. These findings confirm that our approach not only accelerates policy convergence but also enhances safety and adaptability across diverse traffic conditions. In the future, we will explore the application of the TeLL-Drive framework to more dynamic, multi-agent environments and verify its scalability and real-time adaptability through real-vehicle experiments.

REFERENCES

- [1] Long Chen, Yuchen Li, Chao Huang, Bai Li, Yang Xing, Daxin Tian, Li Li, Zhongxu Hu, Xiaoxiang Na, Zixuan Li, et al. Milestones in autonomous driving and intelligent vehicles: Survey of surveys. *IEEE Transactions on Intelligent Vehicles*, 8(2):1046–1056, 2022.
- [2] Szilárd Aradi. Survey of deep reinforcement learning for motion planning of autonomous vehicles. *IEEE Transactions on Intelligent Transportation Systems*, 23(2):740–759, 2020.
- [3] Ammar Haydari and Yasin Yılmaz. Deep reinforcement learning for intelligent transportation systems: A survey. *IEEE Transactions on Intelligent Transportation Systems*, 23(1):11–32, 2020.
- [4] Jiaqi Liu, Peng Hang, Xiao Qi, Jianqiang Wang, and Jian Sun. Mtd-gpt: A multi-task decision-making gpt model for autonomous driving at unsignalized intersections. In *2023 IEEE 26th International Conference on Intelligent Transportation Systems (ITSC)*, pages 5154–5161. IEEE, 2023.
- [5] Guofa Li, Yifan Yang, Shen Li, Xingda Qu, Nengchao Lyu, and Shengbo Eben Li. Decision making of autonomous vehicles in lane change scenarios: Deep reinforcement learning approaches with risk awareness. *Transportation research part C: emerging technologies*, 134:103452, 2022.
- [6] B Ravi Kiran, Ibrahim Sobh, Victor Talpaert, Patrick Mannion, Ahmad A Al Sallab, Senthil Yogamani, and Patrick Pérez. Deep reinforcement learning for autonomous driving: A survey. *IEEE Transactions on Intelligent Transportation Systems*, 23(6):4909–4926, 2021.

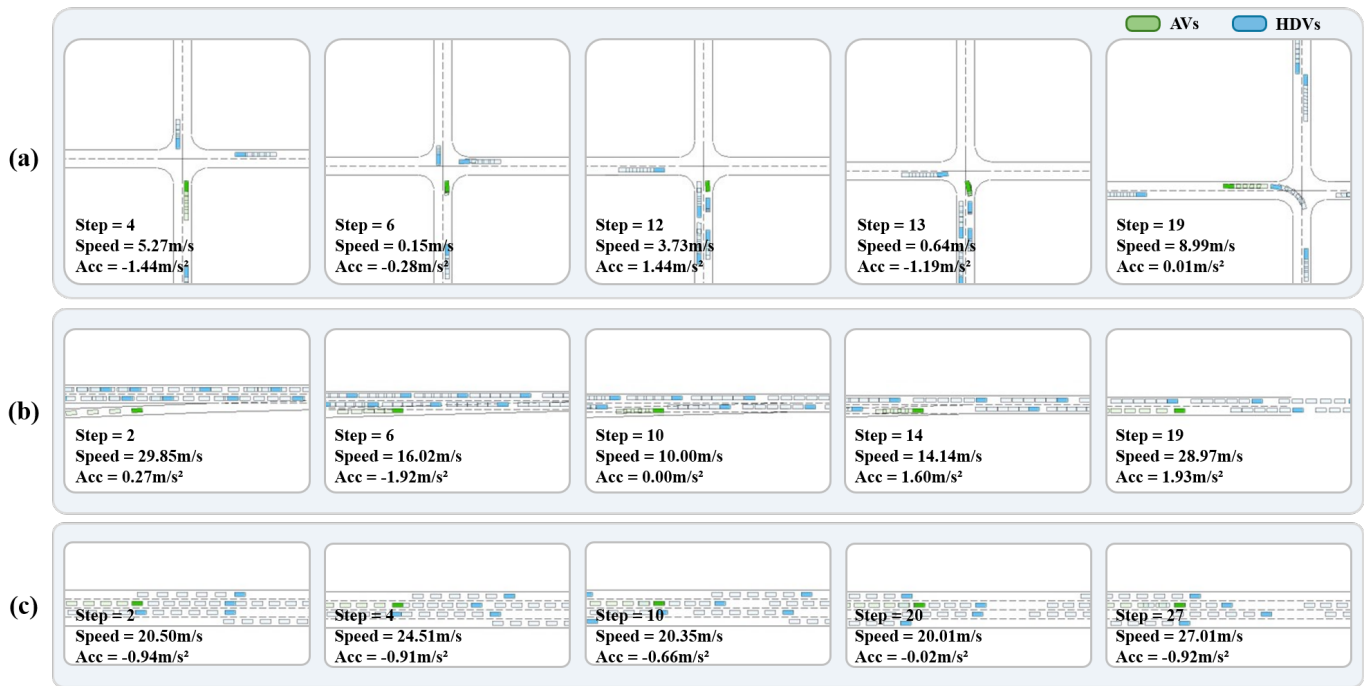


Fig. 8. Test case performance results of TeLL-Drive in three scenarios (a) Unsignalized Intersection, (b) High-Speed Ramp Merging, (c) Four-Lane Adaptive Cruise, where green represents AVs guided by TeLL-Drive and blue represents HDVs.

- [7] Can Cui, Yunsheng Ma, Xu Cao, Wenqian Ye, and Ziran Wang. Drive as you speak: Enabling human-like interaction with large language models in autonomous vehicles. In *Proceedings of the IEEE/CVF Winter Conference on Applications of Computer Vision*, pages 902–909, 2024.
- [8] Zhenhua Xu, Yujia Zhang, Enze Xie, Zhen Zhao, Yong Guo, Kwanyee K Wong, Zhenguo Li, and Hengshuang Zhao. Drivept4: Interpretable end-to-end autonomous driving via large language model. *IEEE Robotics and Automation Letters*, 2024.
- [9] Yaodong Cui, Shucheng Huang, Jiaming Zhong, Zhenan Liu, Yutong Wang, Chen Sun, Bai Li, Xiao Wang, and Amir Khajepour. Drivellm: Charting the path toward full autonomous driving with large language models. *IEEE Transactions on Intelligent Vehicles*, 2023.
- [10] Can Cui, Yunsheng Ma, Xu Cao, Wenqian Ye, Yang Zhou, Kaizhao Liang, Jintai Chen, Juanwu Lu, Zichong Yang, Kuei-Da Liao, et al. A survey on multimodal large language models for autonomous driving. In *Proceedings of the IEEE/CVF Winter Conference on Applications of Computer Vision*, pages 958–979, 2024.
- [11] Jiaqi Liu, Peng Hang, Xiaoxiang Na, Chao Huang, and Jian Sun. Cooperative decision-making for cavs at unsignalized intersections: A marl approach with attention and hierarchical game priors. *IEEE Transactions on Intelligent Transportation Systems*, 2024.
- [12] Xin Xu, Lei Zuo, Xin Li, Lilin Qian, Junkai Ren, and Zhenping Sun. A reinforcement learning approach to autonomous decision making of intelligent vehicles on highways. *IEEE Transactions on Systems, Man, and Cybernetics: Systems*, 50(10):3884–3897, 2018.
- [13] Zhiqing Sun, Sheng Shen, Shengcao Cao, Haotian Liu, Chunyuan Li, Yikang Shen, Chuang Gan, Liang-Yan Gui, Yu-Xiong Wang, Yiming Yang, et al. Aligning large multimodal models with factually augmented rlhf. *arXiv preprint arXiv:2309.14525*, 2023.
- [14] Tianyu Yu, Yuan Yao, Haoye Zhang, Taiwan He, Yifeng Han, Ganqu Cui, Jinyi Hu, Zhiyuan Liu, Hai-Tao Zheng, Maosong Sun, et al. Rlhf-v: Towards trustworthy mlms via behavior alignment from fine-grained correctional human feedback. In *Proceedings of the IEEE/CVF Conference on Computer Vision and Pattern Recognition*, pages 13807–13816, 2024.
- [15] Shiyu Fang, Jiaqi Liu, Mingyu Ding, Yiming Cui, Chen Lv, Peng Hang, and Jian Sun. Towards interactive and learnable cooperative driving automation: a large language model-driven decision-making framework. *arXiv preprint arXiv:2409.12812*, 2024.
- [16] Hao Sha, Yao Mu, Yuxuan Jiang, Li Chen, Chenfeng Xu, Ping Luo, Shengbo Eben Li, Masayoshi Tomizuka, Wei Zhan, and Mingyu Ding. Languageempc: Large language models as decision makers for autonomous driving. *arXiv preprint arXiv:2310.03026*, 2023.
- [17] Daocheng Fu, Xin Li, Licheng Wen, Min Dou, Pinlong Cai, Botian Shi, and Yu Qiao. Drive like a human: Rethinking autonomous driving with large language models. In *Proceedings of the IEEE/CVF Winter Conference on Applications of Computer Vision*, pages 910–919, 2024.
- [18] Licheng Wen, Daocheng Fu, Xin Li, Xinyu Cai, Tao Ma, Pinlong Cai, Min Dou, Botian Shi, Liang He, and Yu Qiao. Dilu: A knowledge-driven approach to autonomous driving with large language models. *arXiv preprint arXiv:2309.16292*, 2023.
- [19] Jiaqi Liu, Chengkai Xu, Peng Hang, Jian Sun, Mingyu Ding, Wei Zhan, and Masayoshi Tomizuka. Language-driven policy distillation for cooperative driving in multi-agent reinforcement learning. *arXiv preprint arXiv:2410.24152*, 2024.
- [20] Danyang Zhang, Lu Chen, Situo Zhang, Hongshen Xu, Zihan Zhao, and Kai Yu. Large language models are semi-parametric reinforcement learning agents. *Advances in Neural Information Processing Systems*, 36, 2024.
- [21] Patara Trirat, Wonyong Jeong, and Sung Ju Hwang. Automl-agent: A multi-agent llm framework for full-pipeline automl. *arXiv preprint arXiv:2410.02958*, 2024.
- [22] Yecheng Jason Ma, William Liang, Guanzhi Wang, De-An Huang, Osbert Bastani, Dinesh Jayaraman, Yuke Zhu, Linxi Fan, and Anima Anandkumar. Eureka: Human-level reward design via coding large language models. *arXiv preprint arXiv:2310.12931*, 2023.
- [23] Zhiyu Huang, Jingda Wu, and Chen Lv. Efficient deep reinforcement learning with imitative expert priors for autonomous driving. *IEEE Transactions on Neural Networks and Learning Systems*, 34(10):7391–7403, 2022.
- [24] Edouard Leurent. An environment for autonomous driving decision-making. <https://github.com/eleurent/highway-env>, 2018.
- [25] Volodymyr Mnih. Playing atari with deep reinforcement learning. *arXiv preprint arXiv:1312.5602*, 2013.
- [26] Volodymyr Mnih. Asynchronous methods for deep reinforcement learning. *arXiv preprint arXiv:1602.01783*, 2016.
- [27] Marco Pleines, Matthias Pallasch, Frank Zimmer, and Mike Preuss. Generalization, mayhems and limits in recurrent proximal policy optimization. *arXiv preprint arXiv:2205.11104*, 2022.
- [28] John Schulman, Filip Wolski, Prafulla Dhariwal, Alec Radford, and Oleg Klimov. Proximal policy optimization algorithms. *arXiv preprint arXiv:1707.06347*, 2017.